Z. Phys. C - Particles and Fields 27, 249-256 (1985)

Zeitschrift für Physik C Particles and Fields

Tagged Two Photon Production of Muon Pairs

PLUTO Collaboration

Ch. Berger, A. Deuter, H. Genzel, W. Lackas, J. Pielorz[a], F. Raupach[b], W. Wagner[c]

I. Physikalisches Institut der RWTH, D-5100 Aachen[d], Federal Republic of Germany

A. Klovning, E. Lillestöl

University, N-5014 Bergen[e], Norway

J. Bürger, L. Criegee, F. Ferrarotto[f], G. Franke, M. Gaspero[f], Ch. Gerke[g], G. Knies, B. Lewendel, J. Meyer, U. Michelsen, K.H. Pape, B. Stella[f], U. Timm, G.G. Winter, M. Zachara[h], W. Zimmermann

Deutsches Elektronen-Synchrotron (DESY), D-2000 Hamburg 52, Federal Republic of Germany

P.J. Bussey, S.L. Cartwright[i], J.B. Dainton, B.T. King, C. Raine, J.M. Scarr, I.O. Skillicorn, K.M. Smith, J.C. Thomson

University, Glasgow[j], G12 8QQ, UK

O. Achterberg[k], V. Blobel, D. Burkart, K. Diehlmann, M. Feindt, H. Kapitza, B. Koppitz, M. Krüger[l], M. Poppe, H. Spitzer, R. van Staa

II. Institut für Experimentalphysik der Universität, D-2000 Hamburg 50[d], Federal Republic of Germany

C.Y. Chang, R.G. Glasser, R.G. Kellogg, S.J. Maxfield, R.O. Polvado[m], B. Sechi-Zorn[a], J.A. Skard, A. Skuja, A.J. Tylka, G.E. Welch, G.T. Zorn

University of Maryland[n], College Park, MD 20742, USA

F. Almeida[o], A. Bäcker, F. Barreiro, S. Brandt, K. Derikum[p], C. Grupen, H.J. Meyer, H. Müller, B. Neumann, M. Rost, K. Stupperich, G. Zech

Universität-Gesamthochschule, D-5900 Siegen[d], Federal Republic of Germany

G. Alexander, G. Bella, Y. Gnat, J. Grunhaus

University of Tel-Aviv[q], Israel

H. Junge, K. Kraski, C. Maxeiner, H. Maxeiner, H. Meyer, D. Schmidt

Universität-Gesamthochschule, D-5600 Wuppertal[d], Federal Republic of Germany

Received 9 November 1984

Abstract. The process $e^+e^- \to e^+e^-\mu^+\mu^-$ has been studied using the PLUTO detector at PETRA. The data agree well with QED calculations to order α^4. Comparison is also made with the predicted leptonic structure function of the real photon using the deep inelastic $e-\gamma$ scattering formalism.

Introduction

The reaction $e^+e^- \to e^+e^-\mu^+\mu^-$ is an example of an α^4 QED process [1]. Studies of this process have mainly been made with nearly real photons [2]. Two experiments have also studied the leptonic photon structure function using highly virtual photons [3, 4]*.

[a] Deceased
[b] Now at Université de Paris Sud, F-91405 Orsay, France
[c] Now at University of California at Davis, Davis, CA 95616, USA
[d] Supported by the BMFT, Federal Republic of Germany
[e] Partially supported by Norwegian Council for Science and Humanities
[f] Rome University, partially supported by I.N.F.N., Sezione di Roma, Italy
[g] Now at CERN, CH-1211 Geneva 23, Switzerland
[h] Institute of Nuclear Physics, PL-30055 Cracow, Poland
[i] Now at Rutherford Appleton Laboratory, Chilton, UK
[j] Supported by the U.K. Science and Engineering Research Council
[k] Now at Texaco Europe Computer Information Systems, D-2000 Hamburg, FRG
[l] Now at Universität Karlsruhe, D-7500 Karlsruhe, FRG
[m] Now at Northeastern University, Boston, MA 02115, USA
[n] Partially supported by the Department of Energy, USA
[o] On leave of absence from Inst. de Fisica, Universidad Federal do Rio de Janeiro, Brasil
[p] Now at BESSY, D-1000 Berlin, Germany
[q] Partially supported by the Israeli Academy of Sciences and Humanities - Basic Research Foundation

* A very preliminary evaluation of the leptonic structure function, using ee and $\mu\mu$, has been given at the Madison Conference, AIP Conference Proceedings **68**, Particles & Fields 22, 576 (1980)

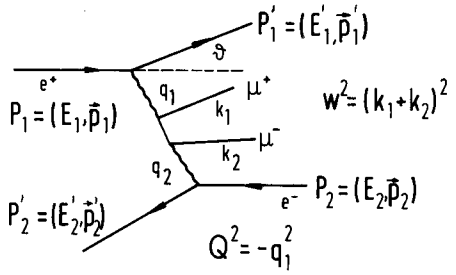

Fig. 1. Kinematics of $\gamma\gamma \to \mu\mu$ in the interaction $e^+e^- \to e^+e^-\mu^+\mu^-$

In this paper we cover the complete range in Q^2 from 0.1 to 100 GeV^2, and present the data in various differential distributions, including the photon structure function. The four momentum squared, $-Q^2$, of the tagged photon is determined from the angle, ϑ, and energy, E', of the scattered electron. The other photon is kept nearly real by restricting the corresponding scattered electron to small angles. The kinematic variables used are defined in Fig. 1.

Measurements were taken using the PLUTO detector at PETRA, with a total integrated luminosity of 38 pb^{-1} at $\sqrt{s} = 35$ GeV ($s = 4E^2_{\text{beam}}$).

The PLUTO Detector and Data Selection

Details of the PLUTO detector can be found in [5]. The following gives a brief description of those components of PLUTO relevant to the present discussion.

(a) A central detector with 13 cylindrical proportional chambers in a magnetic field of 1.65 T provides a momentum resolution of $\sigma(P)/P = 3\,\% \cdot P$ (P in GeV/c) for charged particles.

(b) Barrel and endcap shower counters with imbedded proportional tubes measure the position and energy of electromagnetic showers with angles greater than 280 mrad with respect to the beam.

(c) A muon identifier, with a 1 m thick iron hadron absorber, contains a set of proportional and drift chambers by which track positions are measured at two depths within the absorber.

(d) Two forward spectrometers, each consisting of 5 multi-layer planar drift chambers and a septum magnet, with an integrated magnetic field of 0.2 Tm, give a charged particle momentum resolution of $\sigma(P)/P = 3\,\% \cdot P$. The spectrometers cover a cone from 90 to 250 mrad in polar angle, with two dead regions due to the magnet septa extending to ± 400 mrad in azimuth from the vertical.

(e) The tagging system, which measures the energies and angles of scattered e^+ and e^-, is made up of the following lead-scintillator shower counter components.

1) The Small Angle Tagger (SAT), 19.3 radiation lengths thick, covers the polar region $28 < \vartheta < 60$ mrad. Immediately in front of the calorimeter are proportional wire counters which define the impact position of incident charged particles.

2) The Large Angle Tagger (LAT), 14.5 radiation lengths thick, covers $90 < \vartheta < 260$ mrad. Track reconstruction in the forward spectrometer allows electron-photon separation.

3) The End-cap Tagger (ECT), 10.3 radiation lengths thick, covers $280 < \vartheta < 950$ mrad. The scattering angle ϑ is determined from the electron track as reconstructed in the central detector.

Each of these three systems determines Q^2 with an accuracy of 10 % from measurements of ϑ and E'. The accessible Q^2 ranges are 0.1 to 1.0 for the SAT, 1 to 16 for the LAT, and 10 to 100 GeV^2 for the ECT.

Trigger

A shower of energy >4.0 GeV in the LAT or >2.4 GeV in the ECT triggered the event read-out, independently of other detector components. To avoid unacceptable dead-time due to the high Bhabha scattering rate in the SAT, the SAT trigger required at least one central detector track in coincidence with a shower of energy >6 GeV in the SAT. Uniform trigger efficiency was obtained for central detector tracks with $|\cos\vartheta| < 0.6$ and transverse momentum >200 MeV/c. The trigger efficiency for tagged two prong events was 98 % for ECT or LAT events and 88 % for the SAT tagged events.

Event Selection and Particle Identification

The primary requirements for event selection were that there be at least one tagged electron, and that there be two additional charged particles in the final state.

The tag condition was defined as a SAT shower, or a LAT or ECT shower associated with a reconstructed track. In all cases the shower energy was required to be greater than 6.0 GeV. Cuts in the tag angular acceptance were applied to eliminate edge effects: SAT tags were restricted to $30 < \vartheta < 55$ mrad, and ECT tags to $330 < \vartheta < 680$ mrad. The LAT sample had edge effects in ϑ and φ removed by demanding $100 < \vartheta < 245$ mrad and $|\varphi| > 25°$ away from the vertical, where φ is the azimuthal angle around the beam axis.

The final state was then required to have two oppositely charged tracks (excluding any tags) of

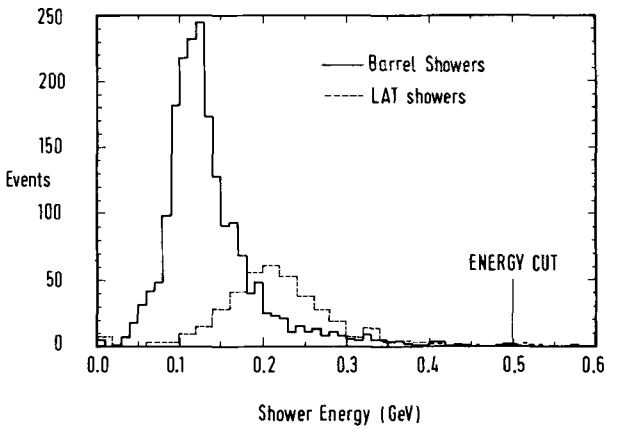

Fig. 2. Shower energy associated with muon tracks

momentum greater than 0.9 GeV/c. Central detector tracks had to be consistent with having their origin at a vertex not more than 40 mm from the beam interaction point. Forward spectrometer tracks were accepted if they gave a track fit through all five chambers.

Following the above selection the two prong sample contained ee, $\mu\mu$ and a few $\pi\pi$ pairs. All tracks were required to have a momentum >0.9 GeV/c to allow separation of electrons and muons using shower energy. If the energy deposited in the shower counter was <0.5 GeV then the track was identified as a muon. To be accepted as a $\mu^+\mu^-$ event both tracks had to be identified as muons. Figure 2, which shows the energy deposition for muons in the Barrel and LAT shower counters, demonstrates that there is a negligible loss of muons and no significant contamination of muon candidates by electrons.

A final selection was made on the invariant mass, W, of the muon system and on the total unassociated neutral energy. Except for the ECT data in Fig. 5c, only invariant masses above 1.2 GeV are used in this analysis, since the data at lower masses contain backgrounds from $\pi^+\pi^-$ production and from $\mu^+\mu^-$ production by virtual bremsstrahlung. These processes are considered in more detail in the next section. In order to reject hadronic events, the total shower energy not associated with a track was required to be <0.1 GeV. This cut was also efficient in reducing backgrounds due to $\tau^+\tau^-$ production. The final data sample, after the W cut, contained 348 SAT, 267 LAT and 28 ECT single tag events consistent with $\gamma\gamma\to\mu^+\mu^-$.

Background Processes

The following backgrounds may be present in the sample of $\mu^+\mu^-$ candidate events:

(i) $\gamma\gamma\to e^+e^-$,
(ii) $\gamma\gamma\to h^+h^-$, where h represents a hadron,
(iii) $\gamma\gamma\to\tau^+\tau^-$,
(iv) $\gamma\gamma\to$multihadrons,
(v) $e^+e^-\to\mu^+\mu^-\gamma$ where the photon simulates a tag,
(vi) $e^+e^-\to$multihadrons $+\gamma$,
(vii) $e^+e^-\to\tau^+\tau^-$,
(viii) $e^+e^-\to e^+e^-\mu^+\mu^-$ by a virtual bremsstrahlung process,
(ix) beam gas interactions.

The $\gamma\gamma\to e^+e^-$ background (i) was determined from a data sample of 615 events containing at least one well-identified electron (excluding the tag) defined as a track associated with a shower of energy >1 GeV and $>|P|/2$. The other track was classified as an electron or a muon as described previously. Of the 22 events in this sample classified as $e-\mu$, 5% were estimated from Monte Carlo studies to be due to $\tau\tau$ production, and the remainder were ascribed to $e-\mu$ misidentification. This could occur if an electron entered a gap between shower detector modules so that only a small fraction of the electron energy was detected. The probability that an electron be identified as a muon was therefore found to be 0.017 ± 0.006. Since the tracks were measured independently the probability that an e^+e^- final state could be identified as a di-muon event was $(3\pm2)\cdot10^{-4}$. This background was therefore neglected.

The $\gamma\gamma\to h^+h^-$ background (ii) may include protons and kaons as well as pions. Data on these processes have been published by the TASSO, PLUTO and CELLO collaborations [6, 7]. Using the procedures described in [7], we have determined this background to be (2.5 ± 1.0)%.

Backgrounds from each of the processes (iii) to (vii) were studied using Monte Carlo event generation with subsequent detector simulation and analysis selections. The reaction $e^+e^-\to\mu^+\mu^-\gamma$ was simulated according to the program of Berends and Kleiss [8]. The annihilation to quark pairs, followed by fragmentation to hadrons, was generated using the program due to Ali et al. [9], modified to include initial state radiation effects as calculated by Berends and Kleiss [10]. These processes can produce a false tag from the radiated photon, from a π^0 decay photon, or from electrons arising from semileptonic decays. The total contamination due to processes (iii) to (vii) ranged from 0.5% for the SAT, to 1.4% for the LAT and 4.5% for the endcap tags.

The beam-gas background was estimated from events whose vertex lay outside the region of collision of the e^+e^- beams and was found to be negligible.

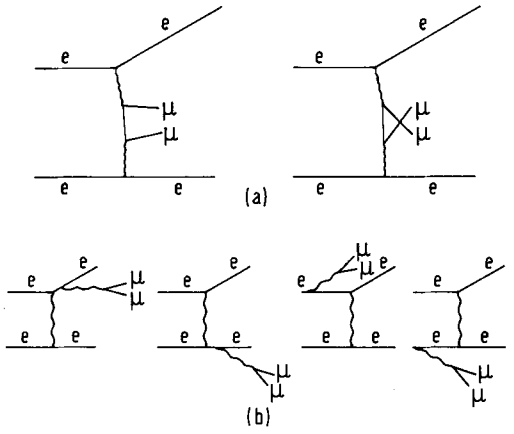

Fig. 3. Feynman diagrams for *a* the two-photon process and *b* the Compton terms

In studying the two-photon process a contamination is possible from inelastic Compton (bremsstrahlung) diagrams (see Fig. 3b), which are characterised [11] by low final state invariant masses and high values of scattering angle of the final state electron. The cross-section for $\mu\mu$ production increases by about 1 % when these diagrams are added to the two-photon diagrams. Although it has been suggested that such a background may be more significant in experiments with limited acceptance [12], a Monte Carlo study of the background Compton processes showed that, for the region $W > 1.2\,\text{GeV}$, they constitute less than 1 % of the signal, even for the highest Q^2 interval.

Comparison of QED Predictions and Data

For the SAT, LAT and ECT data a prediction of the total and differential cross-sections for $\gamma\gamma \to \mu^+\mu^-$ was made using the Vermaseren program [13] which calculates the diagrams shown in Fig. 3a. Radiative corrections to these diagrams were calculated using the the recently-developed Monte Carlo event generator of Berends et al. [14]. In view of the possible sensitivity to a Compton contribution at high Q^2, the ECT data in Fig. 5c were also compared with a Monte Carlo generation [15] which included diagram 3b as well as 3a. The generated events were passed through a simulation program describing the effects of the detector resolution, particle losses, and tracking through magnetic fields.

Total Event Yield

The table below gives the number of SAT, LAT and ECT single tag events found experimentally (DATA) together with the number predicted (MC) using the calculations outlined above, with and without radiative corrections.

	DATA	MC	MC (rad. corr.)
SAT	348 ± 19	373 ± 13	346 ± 14
LAT	267 ± 16	282 ± 12	294 ± 14
ECT	28 ± 5	29 ± 2	34 ± 4

The Monte Carlo numbers include a statistical error and an error of 3 % due to uncertainties in the luminosity. There is good agreement with QED expectations.

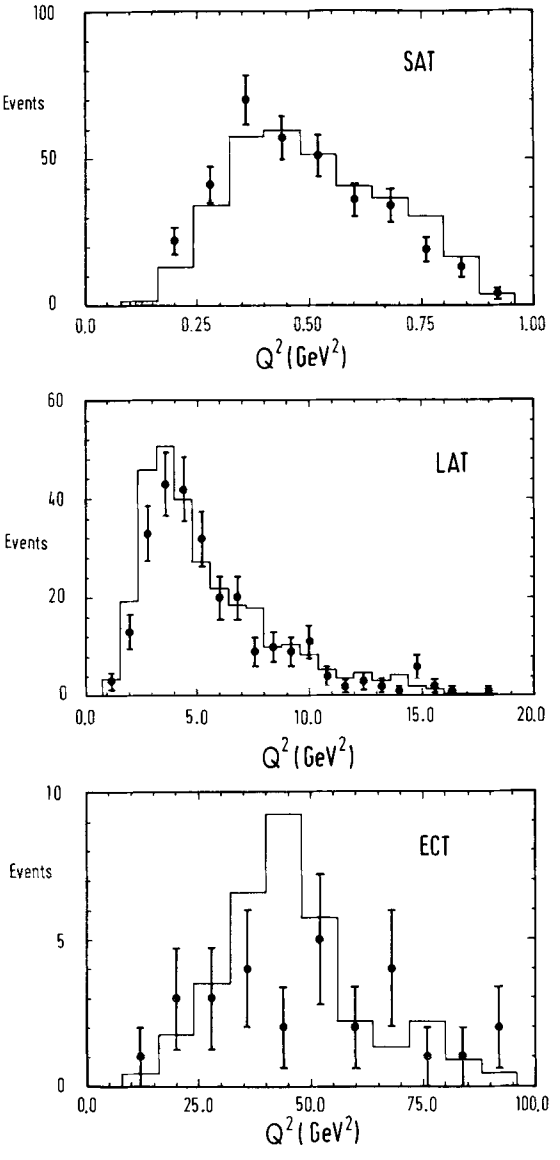

Fig. 4. Q^2 distributions for the SAT, LAT and ECT. The solid line shows the predicted distribution including radiative corrections

Differential Event Yield

Distributions of various tag parameters were compared with Monte Carlo predictions based on QED, including radiative corrections, normalised to the integrated luminosity of the data. All measured distributions agreed well with Monte Carlo predictions. In Fig. 4, for example, Q^2 distributions are given for the three tag categories with, in each case, the prediction from the two photon diagrams with radiative corrections. Figures 5 to 8 show, together with similar theoretical predictions, the differential distributions of W, the angle between the muons, the muon angle with respect to the beam and the muon transverse momentum squared with respect to the gamma-gamma axis in the $\mu\mu$ rest frame.

The agreement between theory and experiment is good, demonstrating the validity of QED. The ECT events in the lowest invariant mass bin in Fig. 5c are attributed to the effect of the Compton terms, and constitute direct experimental evidence for virtual bremsstrahlung contributions to this reaction. Recent results from the PEP-9 collaboration [4] also support this evidence.

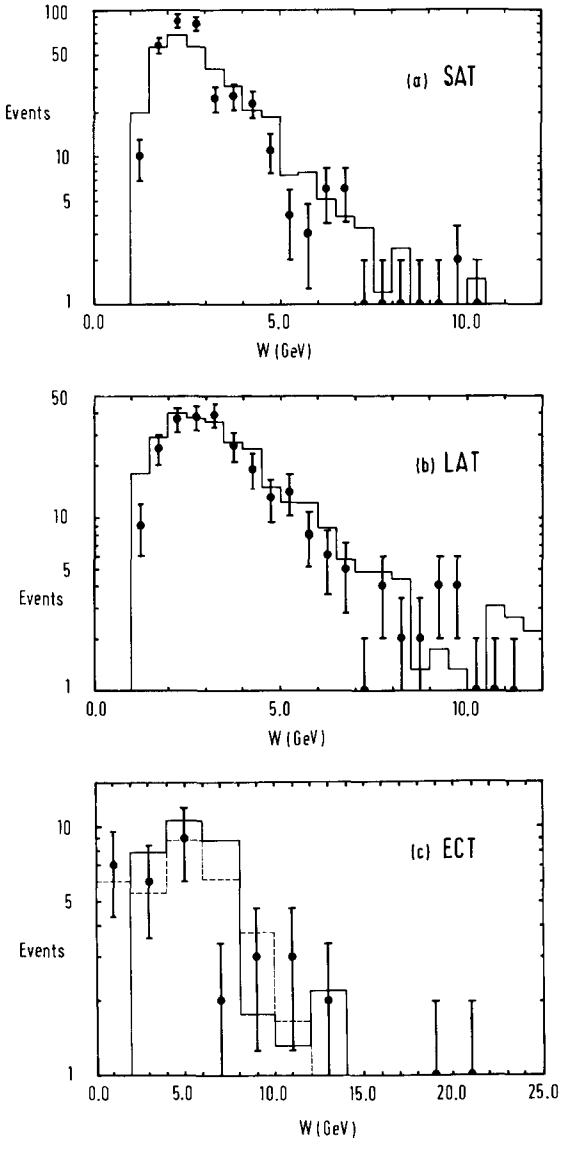

Fig. 5. The effective mass of the muon pair. The solid line is the distribution predicted for the two-photon process. The dotted line in (c) is the prediction from the sum of the two-photon and Compton processes

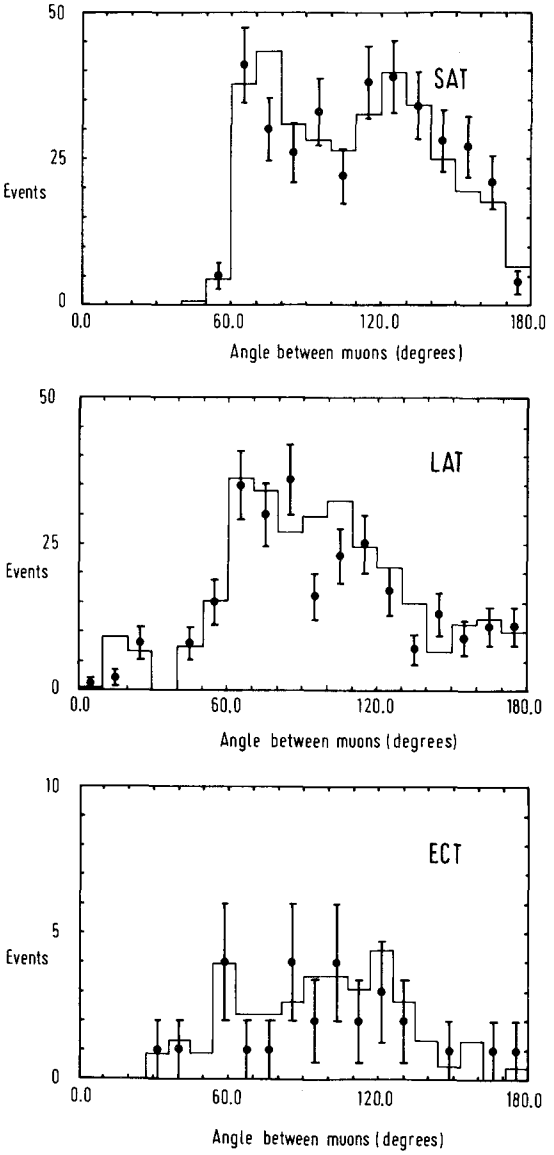

Fig. 6. Angle between the μ^+ and μ^- in the laboratory for $W > 1.2$ GeV. The solid line is the prediction from the two-photon process

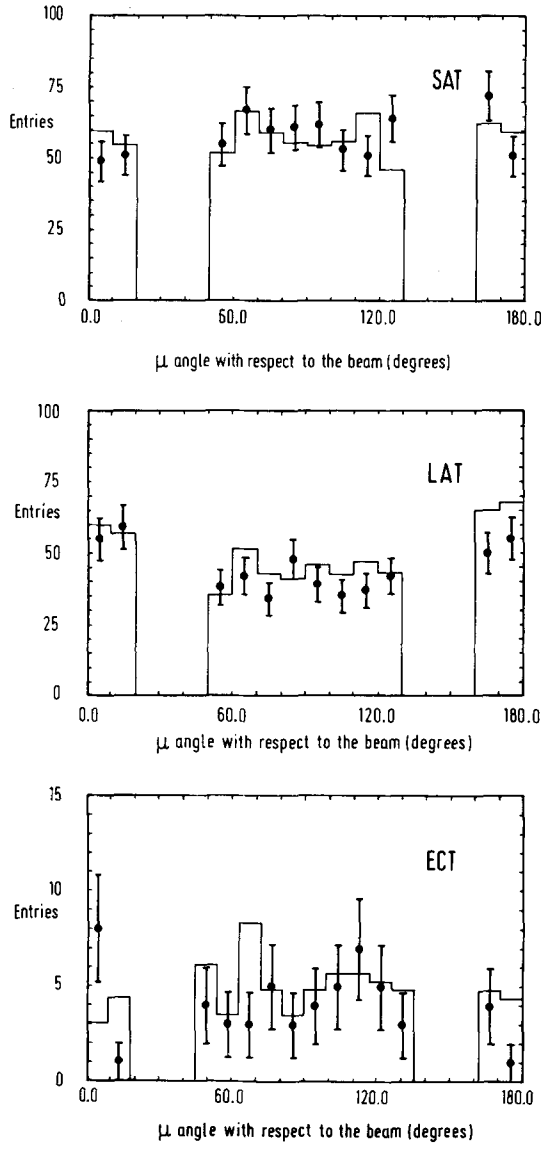

Fig. 7. Polar angle of muons with respect to the e^+e^- beam in the laboratory for $W > 1.2$ GeV. The solid line is the prediction from the two-photon process

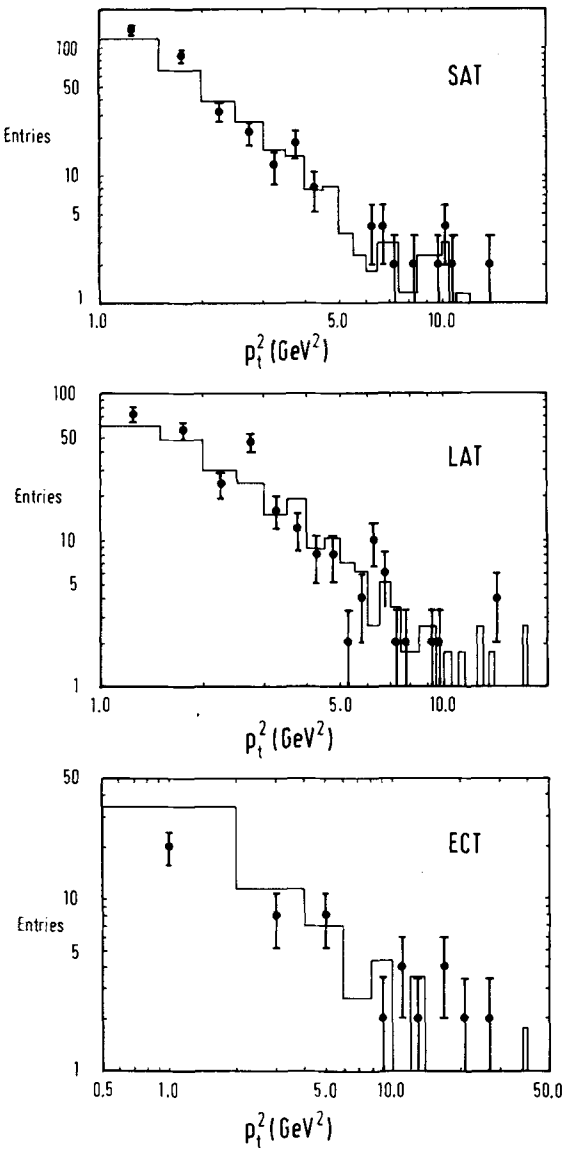

Fig. 8. Distribution of muon transverse momentum squared with respect to the gamma-gamma axis, in the $\mu\mu$ rest frame, for $W > 1.2$ GeV. The solid curve is the two-photon prediction

In spite of the small number of Compton events, further evidence was sought by examining the data for a forward-backward charge asymmetry, which could arise from the interference between muon pairs from the Compton and the $\gamma\gamma$ processes. We define N_f and N_b as the number of muons detected in the forward and backward hemispheres, where the forward hemisphere is defined by the direction of the beam which has the same charge as the muon. The asymmetry A is then defined as $(N_f - N_b)/(N_f + N_b)$, as in [3]. From our data we find $A = (1 \pm 3)\%$. This is in agreement with the value of $(2 \pm 1)\%$ due to asymmetry of the apparatus which we derive from Monte Carlo studies based on zero interference between the diagrams of Figs. 3a and 3b.

Leptonic Structure Function of the Photon

We have also analysed the data in terms of the leptonic structure function of the photon. Neglecting the Compton diagrams, as justified above, the cross section $d\sigma(ee \to ee\mu\mu)$ can be factorised into a cross section $d\sigma(e\gamma \to e\mu\mu)$ multiplied by a flux factor for real photons. The $e-\gamma$ cross-section may be rewritten [11] in terms of the scaling variables x and y, and two leptonic photon structure functions

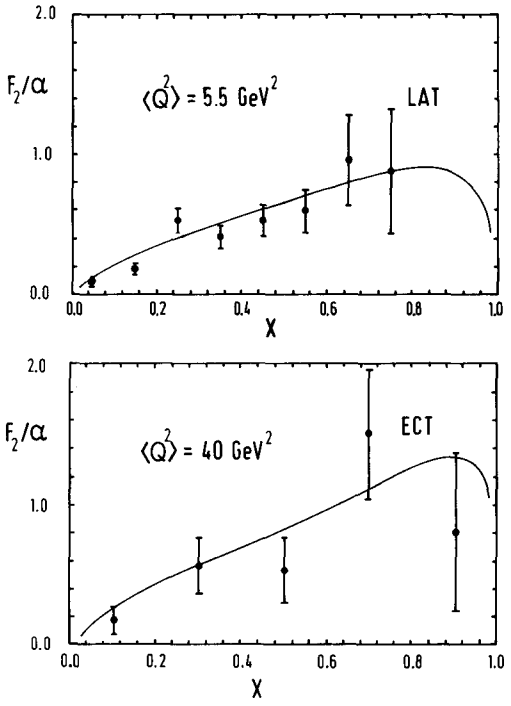

Fig. 9. The leptonic structure function of the photon. The curve is the QED prediction, calculated for the average Q^2 of the LAT and ECT events respectively

$F_L(x, Q^2)$ and $F_2(x, Q^2)$ as

$$d\sigma = (8\pi a^2 E E_\gamma / Q^4)\{(1+(1-y)^2)F_2(x, Q^2) - y^2 F_L(x, Q^2)\}\, dx\, dy \quad (1)$$

where

$$x = Q^2/(Q^2+W^2); \quad y = 1-(E'/E)\cos^2(\vartheta_{tag}/2)$$

and E, E_γ and E' are the beam, target photon and tag energies respectively. In the present experimental arrangement y^2 is small ($\langle y^2 \rangle \sim 0.05$) and therefore the contribution from F_L is negligible; thus this experiment measures $F_2(x, Q^2)$.

To extract the quantity $F_2(x, Q^2)$, Monte Carlo events were generated using a constant $F_2 = \alpha$, $F_L = 0$ and the appropriate $\mu^+\mu^-$ angular distribution. These events simulated the weighting due to the photon luminosity functions and the effects of the detector. The distribution of the data in x divided by that of the Monte Carlo simulation should then result in F_2/α. (The kinematic resolution in the $\mu\mu$ final state is good enough for smearing effects to be ignored.)

Two cross-checks were made to verify the use of this procedure. Firstly, the events generated with the Vermaseren two-photon program were compared with generated events derived from a cross-section of the form (1) using an F_2 calculated from the $\gamma\gamma \to \mu\mu$ QED cross sections [16] and the appropriate centre of mass angular distribution for the muons. No significant difference in event yield or shape of differential distributions was evident, confirming the validity of factorisation. Secondly, events were generated with $F_2 = \alpha x$ and passed through the detector simulation and analysis cuts. F_2 was then determined as described above using a Monte Carlo with a constant F_2. The extracted F_2 agreed with the input F_2, again confirming the validity of the procedures used.

With the condition $W^2 \gg 4M^2$, where W is the invariant mass of the muon pair and M is the muon mass, QED gives

$$F_2(x, Q^2) = (\alpha/\pi)\{x[x^2+(1-x)^2]\ln(W^2/M^2) + 8x^2(1-x) - x + O(4M^2/W^2)\}. \quad (2)$$

Here the mass squared, $-p^2$, of the target photon radiated from the undetected electron is taken to be zero. The extracted F_2/α as a function of x is shown in Fig. 9 for the LAT and ECT data samples. (The SAT data sample covers only the x range below 0.25, and is not shown.) The solid lines show F_2/α from (2), calculated using the mean Q^2 of the respective data samples. The agreement of the data with equation (2) demonstrates again the validity of QED and particularly the assumptions used in the extraction of F_2.

Conclusion

Two photon production of muon pairs has been measured over a Q^2 range of 0.1 to 100 GeV^2. The production of muon pairs is found to be well described by QED calculations of order α^4.

Acknowledgments. We thank the members of the DESY directorate for the hospitality extended to the university groups. We are indebted to the PETRA machine group and the DESY computer centre for their excellent performance during the experiment. We gratefully acknowledge the efforts of all engineers and technicians who have participated in the construction and maintenance of the apparatus.

References

1. R. Battacharya, J. Smith, G. Grammer: Phys. Rev. **D15**, 3267 (1977); J.A. Vermaseren: Proc. of the Int. Workshop on $\gamma\gamma$ Collisions, Amiens, G. Cochard, P. Kessler (Eds.). Berlin, Heidelberg, New York: Springer 1980
2. Mark J Collab. B. Adeva et al.: Phys. Rev. Lett. **48**, 721 (1982); MAC Collab. E. Fernandez et al.: Phys. Rev. **D28**, 2721 (1983); PLUTO Collab. Ch. Berger et al.: Phys. Lett. **94B**, 254 (1980); M. Pohl: Proc. of 5th. Int. Workshop on $\gamma\gamma$ Collisions, Aachen, 1983

3. CELLO Collab. H.J. Behrend et al.: Phys. Lett. **126B**, 384 (1983)
4. PEP-9 Collab. M.P. Cain et al.: University of California (Davis) preprint UCD-840630
5. L. Criegee, G. Knies: Phys. Rep. **83**, 153 (1982); R.G. Kellogg et al.: Internal Report DESY PLUTO 84-04, Sept. 1984; PLUTO Collab. Ch. Berger et al.: Z. Phys. C – Particles and Fields **26**, 199 (1984)
6. CELLO Collab. H.J. Behrend et al.: Z. Phys. C – Particles and Fields **23**, 223 (1984); TASSO Collab. M. Althoff et al.: Phys. Lett. **121B**, 216 (1983); R. Brandelik et al.: Z. Phys. C – Particles and Fields **10**, 117 (1981); R. Brandelik et al.: Phys. Lett. **108B**, 67 (1982)
7. Ch. Berger et al.: Phys. Lett. **137B**, 267 (1984)
8. F.A. Berends, R. Kleiss: Nucl. Phys. **B177**, 237 (1981)
9. A. Ali et al.: DESY Internal Report T-80/01 (1980)
10. F.A. Berends, R. Kleiss: Nucl. Phys. **B178**, 141 (1981)
11. C. Peterson et al.: Nucl. Phys. **B174**, 424 (1980)
12. F.A. Berends, P.H. Daverveldt, R. Kleiss: Z. Phys. C – Particles and Fields **22**, 239 (1984)
13. J.A.M. Vermaseren: Proceedings of the International Workshop on $\gamma\gamma$ Collisions, Amiens (1980)
14. F.A. Berends, R. Kleiss, P.H. Daverveldt: Leiden preprint 1984 (to be published in Nucl. Phys. B)
15. J.A.M. Vermaseren: Private Communication
16. V.M. Budnev, I.F. Ginzburg: Phys. Rep. **15**, 181 (1974)